Published OnlineFirst May 23, 2017; DOI: 10.1158/0008-5472.CAN-17-1098

Microenvironment and Immunology

Cancer Research

Persistent Immune Stimulation Exacerbates Genetically Driven Myeloproliferative Disorders via Stromal Remodeling

Claudio Tripodo[1], Alessia Burocchi[2], Pier Paolo Piccaluga[3], Claudia Chiodoni[2], Paola Portararo[2], Barbara Cappetti[2], Laura Botti[2], Alessandro Gulino[1], Alessandro Isidori[4], Arcangelo Liso[5], Giuseppe Visani[4], Maria Paola Martelli[6], Brunangelo Falini[6], Pier Paolo Pandolfi[7], Mario P. Colombo[2], and Sabina Sangaletti[2]

Abstract

Systemic immune stimulation has been associated with increased risk of myeloid malignancies, but the pathogenic link is unknown. We demonstrate in animal models that experimental systemic immune activation alters the bone marrow stromal microenvironment, disarranging extracellular matrix (ECM) microarchitecture, with downregulation of secreted protein acidic and rich in cysteine (SPARC) and collagen-I and induction of complement activation. These changes were accompanied by a decrease in Treg frequency and by an increase in activated effector T cells. Under these conditions, hematopoietic precursors harboring nucleophosmin-1 (*NPM1*) mutation generated myeloid cells unfit for normal hematopoiesis but prone to immunogenic death, leading to neutrophil extracellular trap (NET) formation. NET fostered the progression of the indolent *NPM1*-driven myeloproliferation toward an exacerbated and proliferative dysplastic phenotype. Enrichment in NET structures was found in the bone marrow of patients with autoimmune disorders and in *NPM1*-mutated acute myelogenous leukemia (AML) patients. Genes involved in NET formation in the animal model were used to design a NET-related inflammatory gene signature for human myeloid malignancies. This signature identified two AML subsets with different genetic complexity and different enrichment in NPM1 mutation and predicted the response to immunomodulatory drugs. Our results indicate that stromal/ECM changes and priming of bone marrow NETosis by systemic inflammatory conditions can complement genetic and epigenetic events towards the development and progression of myeloid malignancy.
Cancer Res; 77(13); 3685–99. ©2017 AACR.

Introduction

Alterations in the bone marrow osteoblastic and vascular niches that nurture hematopoietic stem cells (HSC) are associated with the outgrowth of myeloid cells within a biased leukemic niche (1, 2). Such alterations encompass the adaptation of specific mesenchymal cell populations and the disruption of normal gradients in structural and secreted proteins, including matricellular proteins, cytokines, and chemokines (3). A key regulator of bone marrow stromal changes is the secreted protein acidic and rich in cysteine (SPARC; ref. 4), a matricellular protein in which up- and downregulation has been associated with hematologic neoplasms (2, 5).

Along with remodeling of the bone marrow mesenchymal architecture, myeloid clone expansion changes the cytokine profile of the hematopoietic milieu. Increased levels of proinflammatory cytokines including TNF, IL6, and IL8 have been reported in patients with myeloproliferative neoplasms, myelodysplastic syndromes (MDS), and myeloid leukemia with an unfavorable predicted disease course (6, 7). The induction of an inflammatory state in the myelopoietic parenchyma is mutually linked with the status of the stromal architecture. A defective ECM organization resulting from SPARC deficiency favors the over-activation of myeloid cells (8) and granulocyte immunogenic death via the formation of neutrophil extracellular traps (NET; ref. 5). NETotic death is characterized by the expression of IFN response-related transcriptional programs associated with the induction of inflammation and exacerbation of autoimmune disease, in which NETs contribute as sources of autoantigens and costimulatory signals (9–13). A link has been demonstrated between dysregulated immune stimulation and the occurrence of myeloid malignancies.

[1]Tumor Immunology Unit, Human Pathology Section, Department of Health Science, Palermo University School of Medicine, Palermo, Italy. [2]Department of Experimental Oncology and Molecular Medicine, Fondazione IRCCS Istituto Nazionale Tumori, Milan, Italy. [3]Department of Experimental, Diagnostic, and Experimental Medicine, S. Orsola-Malpighi Hospital, Bologna University School of Medicine, Bologna, Italy. [4]Hematology and Hematopoietic Stem Cell Transplant Center, AORMN, Pesaro, Italy. [5]Department of Hematology, University of Foggia, Foggia, Italy. [6]University of Perugia, Perugia, Italy. [7]Cancer Research Institute and Departments of Medicine and Pathology, Beth Israel Deaconess Medical Center, Harvard Medical School, Boston.

Note: Supplementary data for this article are available at Cancer Research Online (http://cancerres.aacrjournals.org/).

C. Tripodo and A. Burocchi are co-first authors for this article.

M.P. Colombo and S. Sangaletti are co-senior authors for this article.

Corresponding Authors: Mario P. Colombo, Fondazione IRCCS Istituto Nazionale dei Tumori, Via Amadeo 42, Via G. Venezian 1, Milan 20133, Italy. Phone: 3902-2390-2252; Fax: 3902-2390-2630; E-mail: mariopaolo.colombo@istitutotumori.mi.it; and Sabina Sangaletti, sabina.sangaletti@istitutotumori.mi.

doi: 10.1158/0008-5472.CAN-17-1098

Published OnlineFirst May 23, 2017; DOI: 10.1158/0008-5472.CAN-17-1098

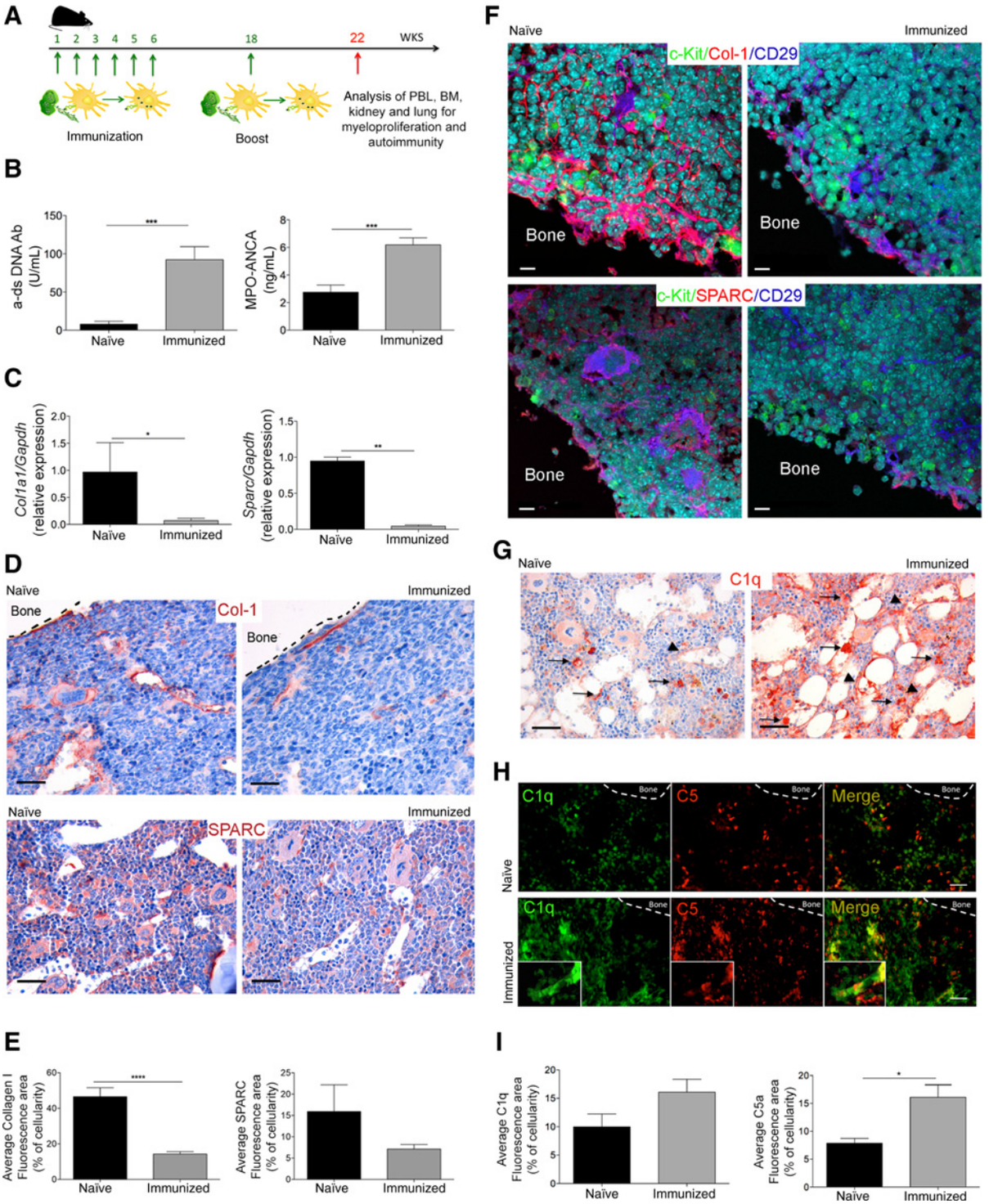

Figure 1.

Chronic immune stimulation induces stromal changes in the bone marrow (BM). **A,** Schematic representation of NET-loaded DC-based immunization protocol. **B,** Quantification of anti-dsDNA autoantibodies and MPO-ANCA levels in immunized and control mice. Data are expressed as U/mL of IgG for anti-dsDNA or as ng/mL of IgG for MPO-ANCA ($n = 10$/each group; ***, $P < 0.001$, Mann–Whitney test). **C,** Expression of *Sparc* and *Col1a1* in total bone marrow cells isolated from immunized and control mice. The fold change in the expression of the target genes relative to the internal control gene (GAPDH) is shown ($n = 5$; *, $P < 0.05$, Mann–Whitney test). **D,** Representative IHC analysis of type I collagen and SPARC shows the reduction of both ECM molecules in the bone marrow of immunized mice. Scale bars, 50 μm. **E,** Quantitative analysis of collagen type I and SPARC in immunofluorescence images as detailed in the Supplementary Methods. (*Continued on the following page.*)

Published OnlineFirst May 23, 2017; DOI: 10.1158/0008-5472.CAN-17-1098

Large-scale epidemiologic studies have shown that the history of chronic autoinflammatory or autoimmune diseases is correlated with increased incidence of MDS or acute myeloid leukemia (AML; ref. 14); however, the role of systemic immune activation in the pathobiology of myeloid malignancies remains unknown. The highest risk of development of MDS and AML has been reported in patients with autoimmune diseases in which NETs have a recognized pathogenic role, for example, systemic lupus erythematosus and antineutrophil cytoplasmic antibody (ANCA)-related vasculitis (9, 15).

In this study, we investigated whether a persistent immune stimulation can change the bone marrow stromal microenvironment and affect hematopoietic precursor proliferation. We identified a novel regulation of myeloid cell expansion involving the crosstalk between the immune cells and stromal components of the bone marrow microenvironment. Such crosstalk is proposed to be relevant in explaining the link between systemic immune activation and myeloid neoplasms.

Materials and Methods

Mice

hMPR8-NPMc$^+$ transgenic mice (*B6. Tg<hMRP8-NPMc> Ptprc<b>tg/J*), hereafter referred as *NPMc*, were obtained by backcrossing (C57BL/6J × CBA) F1-*hMRP8-NPMc* mice to C57BL/6 (B6. *Ptprc<b>*). The bone marrow of *Trif*$^{+/-}$ mice was kindly provided by Dr. Garlanda (Humanitas Clinical and Research Center, Milan, Italy). All experiments involving animals described in this study were approved by the Ministry of Health (authorization number 10/11). The protocol describing the immunization of WT and *NPMc* mice with NET-loaded DCs is described in the Supplementary Data.

Human and murine bone marrow histology, immunohistochemistry, and immunofluorescence

Histologic, histochemical, and immunofluorescence analyses of murine and human bone marrow samples were performed as previously described (2, 5) and detailed in the Supplementary Data. For *in situ* histopathologic analyses of human bone marrow specimens, the bone marrow biopsies from 12 patients with autoimmunity-associated peripheral cytopenias were selected from the archives of the Department of Hematology, University of Foggia, Foggia, Italy, and the Department of Health Sciences, University of Palermo, Palermo, Italy. Patient characteristics are listed in Supplementary Table S1.

Bone marrow and spleen FACS analysis of hematopoietic precursors

Briefly marrow and spleen cell suspensions were stained with a pool of antibodies for Lin positive markers, including CD3, CD11b, CD45R, Ly6G, CD4, CD8, and Ter-119, and stem cell and progenitor cell markers, including CD117 (c-Kit), CD34, and CD16/CD32. Progenitors were identified according to their expression of CD34 and CD16/CD32 within the gate of Lin$^-$CD117$^+$ cells. Bone marrow, spleens, and PBL samples were also evaluated for granulocyte enrichment by staining cell suspensions with mAbs against CD11b, Ly6G, and CD45, followed by FACS analysis. All antibodies were purchased from eBioscience. Samples were acquired on an LSR II (BD Biosciences).

Immunization of WT and NPMc preleukemic mice with NET-loaded dendritic cells

Inflammatory PMNs (IFNγ/TNF-treated), prone to dye of NETosis, were obtained from agar plugs subcutaneously injected into C57BL/6 mice, as previously described (9). In particular, PMN were seeded onto coated tissue culture dishes in IMDM 2% FCS, allowed to adhere for 30 minutes and added with myeloid dendritic cell (mDC; 1:1; PMN:DC) for 16 hours. During this period NETs are induced and transfer their component to mDCs (9). Dendritic cell (DC) were isolated from the coculture via positive selection, counted and injected intraperitoneally (2.5–5 × 10^6 cells, once a week for a total of six injections) into naïve mice. Three months after the last immunization, mice underwent a boosting immunization. Autoimmunity was evaluated starting 1 month after the boost by measuring the titer of ANCA and dsDNA autoantibodies using specific ELISA kits (MPO-ANCA IgG, ELISA Kit from Cusabio and mouse anti-dsDNA antibody ELISA Kit from Alpha Diagnostic International).

Qualitative and quantitative evaluation of NET formation

For *ex vivo* isolated neutrophils, spontaneous NETosis was evaluated by seeding bone marrow-derived PMNs onto poly-D-lysine–coated glasses in 2% FCS-IMDM in presence or absence of PMA (16). To quantify NETosis and to distinguish NETosis from apoptosis, the cell-impermeable DNA dye Sytox green, was added to PMNs such to measure the size of the released nuclear contents from micrographs using the software-assisted technique, according to Metzler and colleagues (17). To assess NET formation *in vivo* in murine and human bone marrow biopsies, confocal microscopy analysis was performed by staining with mAbs to murine or human-MPO (from Millipore and Novocastra, respectively) and anti-Histone H3 (citrulline R2+R8+R17, from Abcam), followed by staining with Alexa Fluor 546-conjugated goat anti-rabbit or goat anti-mouse secondary antibodies (Invitrogen Molecular Probes). Nuclei were counterstained with Draq5 or Dapi. To evaluate nucleophosmin (NPM) relocalization onto the NET threads, PMA-induced NETs (obtained from splenic WT- and *NPMc*-PMN treated 16 hours with PMA) were sequentially stained with mAb to nucleophosmin (18) and MPO (Millipore) or PR3 (Millipore). The NET-DNA was counterstained with Draq5.

In vitro cultures of Lin$^-$c-Kit$^+$ hematopoietic cells

Lin$^-$c-Kit$^+$ cells were FACS-sorted from the bone marrow of *NPMc* or control mice (BD, FACSAria), stained with carboxyfluorescein succinimidyl ester (CFSE) and added to PMNs undergoing NETosis [inflammatory PMNs from agar plugs (9) or PMA-treated

(*Continued*.) **F,** Representative triple confocal microscopy analysis of type I collagen or SPARC, together with CD29 and c-Kit performed on bone marrow sections from immunized and control mice. The image shows the reduction of type I collagen and SPARC expression in mesenchymal (CD29$^+$) cells of the osteoblastic niche that is enriched in hematopoietic (c-Kit$^+$) hematopoietic precursors. Scale bars, 10 μm. **G,** IHC of C1q in bone marrow sections from immunized and control mice showing an increase in vascular (arrows) and stromal (arrowheads) C1q expression in immunized mice. **H,** Representative double immunofluorescence analysis showing that the increased C1q induction in the bone marrow of immunized mice is associated with an increase in the stromal deposition of C5a. **I,** Quantitative analysis of C1q and C5a in immunofluorescence images as detailed in Supplementary Methods.

Published OnlineFirst May 23, 2017; DOI: 10.1158/0008-5472.CAN-17-1098

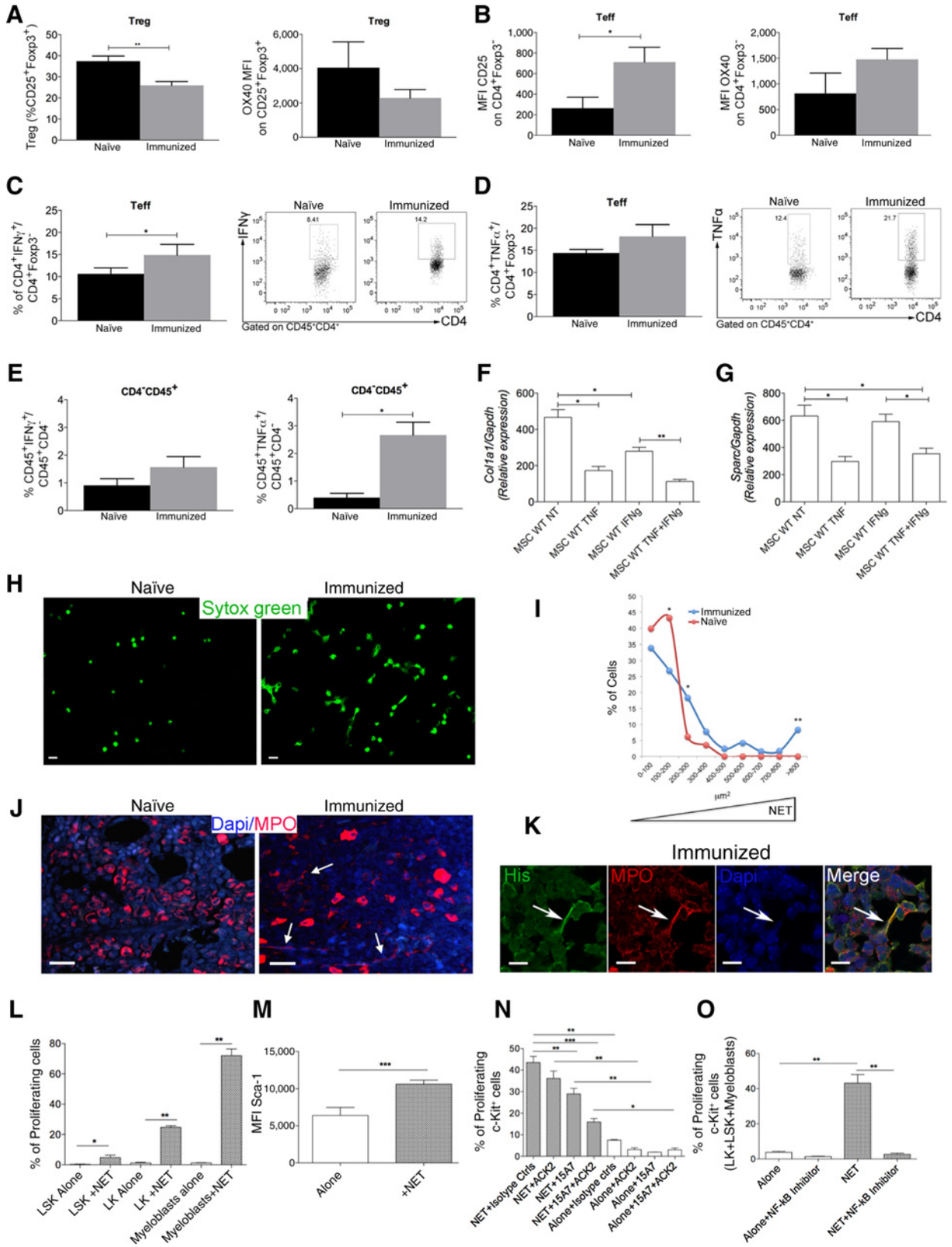

Published OnlineFirst May 23, 2017; DOI: 10.1158/0008-5472.CAN-17-1098

PMNs]. The coculture was performed in StemSpan H3000 medium (Stem Cell Technologies), without adding any other supplement. After 72 hours of coculture, cells are harvested and the c-Kit$^+$ cell fraction, which comprised c-Kit$^+$Sca$^+$GR-1$^-$ early progenitors, c-Kit$^+$Sca$^-$GR-1$^-$ committed precursors (mostly GMP), and c-Kit$^+$Sca$^-$GR-1$^+$ myeloblasts, was analyzed for proliferation. Proliferation was read out by measuring dilution of the CFSE dye (19).

Gene expression profile analysis

Gene expression profile (GEP) analysis was performed in a panel of primary hematopoietic malignancies, including AML (AN = 100), chronic myelogenous leukemia (CML, $N = 50$), MDS ($N = 50$), and in a panel of healthy bone marrow samples ($N = 30$), which were randomly selected among those included in a large multicentric GEP study available on GEO database (GSE13159; refs. 20, 21). We also analyzed 461 AML cases for which gene expression data and information on the *NPM1* status (mutated vs. wild type) were available (GEO Access: GSE6891; refs. 22, 23) and 15 AML cases included in a phase II clinical trial testing the combination of lenalidomide and cytarabine (Len-Ara) and for which our group previously generated GEP (24). Each case was assigned to either group 1 or 2 based on the expression of the NET-related inflammatory signature. A detailed description of the analysis performed is provided in the Supplementary Data.

Results

Systemic autoimmunity induces modifications in the bone marrow stromal and immune cell compartments

To investigate how systemic autoimmunity could affect bone marrow stroma remodeling, naïve C57BL/6 mice were repeatedly immunized by intraperitoneal injections of mDC loaded with NET components (Fig. 1A and Supplementary Data). As previously shown (9), immunized mice developed serum autoantibodies and ANCA-associated autoimmune vasculitis in the kidney and lung parenchyma (Fig. 1B; Supplementary Fig. S1A and S1B). Compared with naïve mice, the bone marrow of immunized mice showed a significant decrease in the levels of type I collagen and SPARC, as assessed by semiquantitative PCR (Fig. 1C), IHC (Fig. 1D), and *in situ* immunofluorescence (Supplementary Fig. S1C). The decrease in type I collagen and SPARC was particularly evident in CD29$^+$ stromal cells lining the osteoblastic (OB) niche, which is enriched in c-Kit$^+$ precursors (Fig. 1F). Moreover, stromal and endothelial bone marrow cells showed increased C1q expression, which was associated with C5a (Fig. 1G–I), suggesting activation of the complement cascade. Finally, a trend in the induction of P-selectin expression was also observed in the bone marrow of immunized mice (Supplementary Fig. S1D–S1F).

Foxp3$^+$ Treg cells are typically either depleted or skewed toward inflammatory Th1 or Th17 cells under autoimmune conditions (25). In the bone marrow of naïve mice, nearly 30% of CD4$^+$ T cells were Foxp3$^+$ Treg cells, a frequency much higher than that of the other lymphoid organs, where Treg cells accounted for 5% to 15% of total CD4$^+$ T cells (Supplementary Fig. S1G and S1H). In contrast, in the bone marrow of immunized mice the frequency of Treg cells was significantly reduced (Fig. 2A). Also reduced in this subset was the expression of OX40 (26), a marker of activation (Fig. 2A). On the contrary, the expression of CD25 and OX40 on Teff cells was increased (Fig. 2B) together with their production of IFNγ and TNF (Fig. 2C and D). In immunized mice, TNF and IFNγ were also induced in CD45$^+$ cells other than T lymphocytes (Fig. 2E).

To test the existence of a link between the TNF- and IFNγ-rich inflammatory milieu and stromal ECM modifications, bone marrow-MSCs were isolated from the bone marrow of naïve mice and stimulated 24 hours with IFNγ, TNF, or both. Semiquantitative PCR analysis showed that these stimuli, mostly when in combination, significantly decrease the expression of *col1a1* and *Sparc* in bone marrow-MSCs (Fig. 2F and G).

Collectively, these results show that systemic immune activation modifies the bone marrow stromal microenvironment and changes the immune cell composition from immune-regulatory to proinflammatory.

Figure 2.

A proinflammatory bone marrow microenvironment supports NET formation, thereby promoting hematopoietic precursor proliferation. **A,** Reduced frequency of CD4$^+$CD25$^+$Foxp3$^+$ Tregs and their reduction in OX40 fitness marker expression (MFI, mean fluorescent intensity) in bone marrow (BM) of immunized (gray bar) compared with naïve (black bar) mice. **B,** Activation of CD4$^+$Foxp3$^-$ Teff upon immunization evaluated in terms of CD25 and OX40 expression. **C** and **D,** Activation of CD4$^+$Foxp3$^-$ Teff upon immunization evaluated as IFNγ and TNF secretion. The frequency of IFNγ- and TNF-secreting cells was evaluated within the gate of CD4$^+$ and Foxp3$^-$ cells as shown in the relative representative gating strategy. **E,** IFNγ and TNF secretion by non-CD4 leukocytes in the bone marrow of naïve (black bar) and vaccinated (gray bar) mice. Data are representative of three independent experiments, each including five mice per groups; statistical analysis: Student's *t* test, *, $P < 0.05$; **, $P < 0.01$. **F** and **G,** Expression of *Col1a* and *Sparc* genes in bone marrow-MSC stimulated or not with IFNγ, TNF, or their combination. The fold change in expression of the target genes relative to the internal control gene (GAPDH) is shown. **H,** *Ex vivo* spontaneous NET formation by PMNs isolated from the bone marrow of immunized or control mice. Spontaneous NET formation was evaluated by seeding bone marrow–isolated PMNs into poly-D-lysine–coated glasses in presence of the DNA-dye Sytox green. Scale bars, 10 μm. **I,** Quantification of NET formed by bone marrow-PMNs isolated from immunized mice. Nuclear area of bone marrow PMN from naïve and immunized mice is plotted against the percentage of SYTOX-positive cells corresponding to a given nuclear area. PMN undergoing NETosis are characterized by broad range of nuclear areas, whereas apoptotic neutrophils show smaller nuclear areas. Quantification shows that PMN from immunized mice make more NET in comparison to PMN from naïve mice. Experiments comparing the two types of bone marrow PMN were repeated three times with PMN from at least three donor mice each. Number of nuclei analyzed/experiment = 100. **J,** Immunofluorescence for MPO performed on bone marrow sections from immunized and naïve mice showing the presence of extracellular MPO threads, which is associated with NET formation (arrows), in bone marrow sections from immunized mice. In naïve mice, MPO staining was confined to the cytoplasmic area of myeloid cells. Scale bars, 50 μm. **K,** Representative confocal microscopy analysis showing the colocalization of citrullinated histone H3, MPO, and DAPI in extracellular traps of bone marrow from immunized mice. Scale bars, 10 μm. **L,** To determine the role of NET in hematopoietic precursor proliferation, FACS-sorted c-kit$^+$ bone marrow cells were stained with the proliferation dye CFSE and cocultured with NET. The proliferative effect of NETs was analyzed in the different fractions of c-Kit$^+$ hematopoietic cells (see Supplementary Fig. S2B for representative plots; $n = 10$ per group; **, $P < 0.01$, Mann–Whitney test). **M,** Expression of Sca (MFI) in c-Kit$^+$Sca$^+$GR-1$^-$ early progenitors cocultured or not with NET ($n = 10$ per group; **, $P < 0.01$, Mann–Whitney test). **N,** Proliferation of CFSE-labeled FACS-sorted Lin$^-$c-Kit$^+$ cells to NETs in presence of mAbs blocking SCF-1 (ACK2) or IL6 (15A7) or isotype controls ($n = 10$ per group, excluding controls; for controls $n = 5$ per group; *, $P < 0.05$; **, $P < 0.01$; ***, $P < 0.001$; Mann–Whitney test). **O,** Inhibition of NET-induced Lin$^-$c-Kit$^+$ cell proliferation by a specific NF-κB inhibitor (InSolution NF-κB activation inhibitor, Calbiochem; $n = 6$ per group; **, $P < 0.01$, Mann–Whitney test). NF-κB inhibition completely abrogated the NET-induced proliferation of c-Kit$^+$ cells.

Published OnlineFirst May 23, 2017; DOI: 10.1158/0008-5472.CAN-17-1098

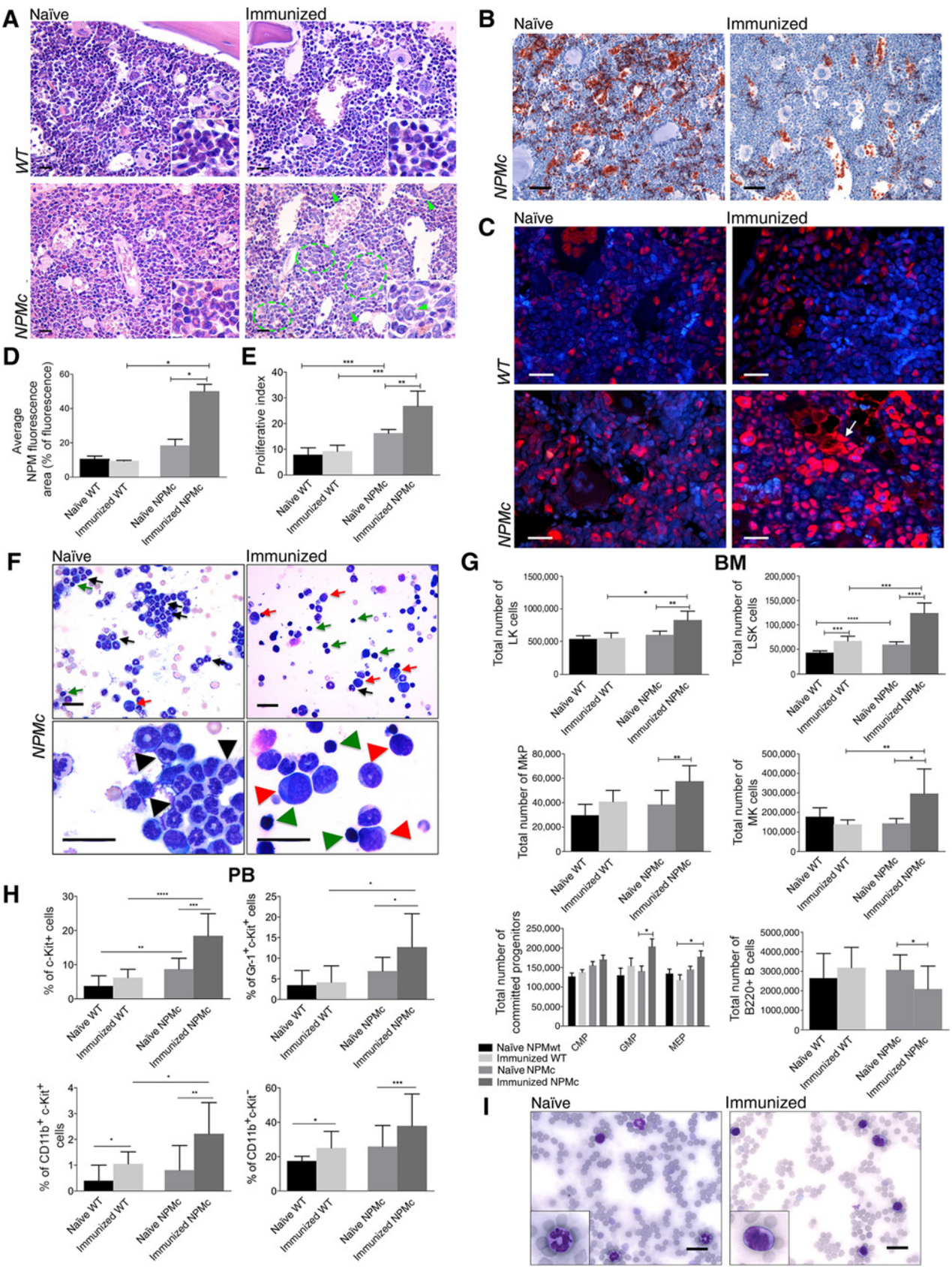

Published OnlineFirst May 23, 2017; DOI: 10.1158/0008-5472.CAN-17-1098

NET formation in a proinflammatory bone marrow microenvironment promotes HSC proliferation via IL6, SCF, and NF-κB activation

TNF, IFNγ (9), and complement factors (27) are major drivers of NET formation. In a context of defective ECM molecules (collagens and SPARC), their NET-inducing capacity increases because of the lack of inhibitory signals that are provided by collagens on activated PMN (5). Therefore, we investigated whether induction of systemic autoimmunity affected NET formation by bone marrow cells. Immunized mice showed increased NET formation, as assessed *ex vivo* by measuring the capacity of bone marrow–derived polymorphonuclear leukocytes (PMN) to undergo spontaneous NETosis (Fig. 2H and I) as well as *in situ* by immunoflourescence (Fig. 2J) and confocal microscopy (Fig. 2K).

We then investigated the capacity of NETs to affect the proliferation of bone marrow hematopoietic cells. $Lin^-c\text{-}Kit^+$ (LK) hematopoietic cells were sorted from the bone marrow, stained with carboxyfluorescein succinimidyl ester (CFSE) and cocultured with NETs in conditions enabling HSC maintenance and differentiation toward myeloid lineages. As a source of NETs, we used PMNs isolated from *in vivo* inflammatory foci that undergo spontaneous NETosis dependent on TNF and IFNγ priming (9). In some experiments, PMA-treated NETotic PMNs were used as positive controls (28). Starting from 72 hours of coculture, NETotic, but not apoptotic, necrotic, or naïve PMNs, significantly enhanced the proliferation of $c\text{-}Kit^+$ bone marrow cells (Supplementary Fig. S2A). An in depth analysis showed that NET specifically enhanced the proliferation of $c\text{-}Kit^+Sca^+GR\text{-}1^-$ early progenitors (LSK), $c\text{-}Kit^+Sca^-GR\text{-}1^-$ (LK) committed precursors (mostly GMP), and $c\text{-}Kit^+Sca^-GR\text{-}1^+$ myeloblasts (Fig. 2L, representative gating strategy in Supplementary Fig. S2B). Moreover, NETs sustained the expression of Sca-1 in $c\text{-}Kit^+Sca^+Gr\text{-}1^-$ early progenitor cells, which is crucial for HSC self-renewal and proliferation (Fig. 2M).

Investigating the mechanism involved in NET-induced proliferation of $c\text{-}Kit^+$ cells, we first excluded the involvement of TLRs as sensor of the NET DNA-backbone (Supplementary Fig. S2C and S2D). Considering that the proliferation of $c\text{-}Kit^+$ cells induced by NETs was diminished, but not abrogated, by the interposition of a transwell membrane (Supplementary Fig. S2E and S2F), we evaluated the role of soluble mediators. Stem cell factor (SCF) and IL6 are known to promote hematopoietic cell renewal and clonogenic capacity through NF-κB (29). MAbs blocking either the IL6 receptor (15A7) or c-Kit (ACK2) strongly inhibited NET-induced proliferation of $c\text{-}Kit^+$ hematopoietic cells, an effect magnified by the simultaneous blockade of both receptors (Fig. 2N). Pharmacological inhibition of NF-κB had a comparable effect (Fig. 2O), being NF-κB the main transducer of IL6R on hematopoietic precursors (30). These data indicate that NET inflammatory pressure exerted on $c\text{-}Kit^+$ hematopoietic cells through IL6 and SCF release confers a proliferative advantage to hematopoietic precursors.

NET-associated immune stimulation exacerbates NPM1 mutation-driven myeloproliferation *in vivo*

We then investigated whether NET-induced stimulation of hematopoietic precursors could impact on the proliferation of myeloid cells under myeloproliferative conditions *in vivo*. *NPMc* transgenic mice carry the human mutated *NPMc* under a myeloid-specific promoter and are prone to develop an indolent myeloproliferation, in which mature myeloid cells expand without progressing towards myelodysplasia or leukemia (31). Induction of systemic autoimmunity in *NPMc* transgenic mice elicited modifications in the bone marrow microenvironment that mirrored those observed in immunized WT mice (Supplementary Figs. S3 and S4) and included *in situ* formation of NETs (Supplementary Fig. S5A).

Compared with naïve *NPMc* mice, a significantly higher percentage of immunized *NPMc* mice developed a myeloproliferative disorder at approximately 12 months of age (60% vs. 25%, $P < 0.05$). In these mice, bone marrow histopathology revealed an exacerbated myelodysplastic/myeloproliferative phenotype with a left-shift of myelopoiesis, clustering of atypical myeloid precursors, dysmegakaryopoiesis, and signs of intravascular hematopoiesis (Fig. 3A). Paralleling the exacerbated myeloproliferation the bone marrow of immunized NPMc mice showed a significant difference in the density of bone marrow erythroid colonies highlighted by TER-119 immunostaining (Fig. 3B).

Consistently, the frequency of cytoplasmic NPM-expressing elements and of proliferating Ki67-expressing myeloid elements in the bone marrow of immunized *NPMc* mice was significantly higher as compared with naïve *NPMc* controls (Fig. 3C–E). Moreover, bone marrow smears of immunized *NPMc* mice showed an increase in immature forms of myeloid cells with atypical morphology (Fig. 3F, red arrows), a concomitant decrease in segmented mature granulocytes (black arrows), and an increase in lymphoid elements (green arrows). Flow cytometry analysis of the bone marrow showed a significant expansion in the fraction of hematopoetic precursors (LK and LSK) and committed

Figure 3.

NET-associated immune stimulation cooperates the with NPMc background in shaping the myeloproliferative phenotype. **A,** Representative bone marrow histopathology showing hematopoietic parenchyma of WT and *NPMc* naïve and immunized mice. *NPMc* transgenic mice exhibit myeloproliferative features with prominent mature granulocytopoiesis. Upon immunization, the exacerbated myelopoiesis of *NPMc* mice becomes dysplastic with significant left-shift of myel- and megakaryocytopoiesis and increase in atypical myeloid precursor clusters (arrowheads, inset). Signs of intravascular hematopoiesis are evident in these samples (dashed green line). Scale bars, 50 μm. **B,** IHC analysis for the erythroid Ter119 marker on bone marrow paraffin sections from immunized and naïve *NPMc* mice. Scale bars, 100 μm. **C,** Representative IF analysis for NPM performed on bone marrow (BM) paraffin sections from naïve or immunized WT and *NPMc* mice. Scale bars, 50 μm. **D,** Quantitative analysis of NPM immunofluorescence performed on five bone marrow sections from naïve and immunized *NPMc* or WT mice. Statistical analysis: Student *t* test; *, $P < 0.05$. **E,** Quantification of the Ki67 proliferative index in bone marrow biopsies from immunized and naïve *NPMc* or WT mice ($n = 5$ per group; statistical analysis: Student *t* test; **, $P < 0.01$;***, $P < 0.001$). **F,** bone marrow smears of immunized *NPMc* mice showed an increase in myeloid blasts with atypical morphology (red arrows), a concomitant decrease in segmented mature granulocytes (black arrows), and an increase in lymphoid elements (green arrows) compared with naïve *NPMc* mice, which showed a predominance of segmented granulocytes and rare blasts. Scale bars, 20 μm. **G,** Bone marrow FACS analyses showing the total amount of $Lin^-c\text{-}Kit^+$ and $Lin^-Sca1^+Kit^+$ precursor cells and myeloid progenitors (GMP) in the bone marrow of immunized *NPMc* mice. The induction of megakaryocytes (Mk) and their progenitors (MkP) was also observed ($n = 10$ per group; statistical analysis: Student *t* test; *, $P < 0.05$; **, $P < 0.01$; ***, $P < 0.001$). The exacerbated myelopoiesis of immunized *NPMc* mice was associated with a slight but significant decrease in $B220^+$ lymphoid cells. **H,** PB FACS analysis showing the increased percentage of the overall circulating $c\text{-}Kit^+$ cells, myeloblasts ($Gr\text{-}1^+c\text{-}Kit^+$ and $CD11b^+c\text{-}Kit^+$), and mature $CD11b^+$ myeloid cells in immunized *NPMc* transgenic mice. **I,** Representative PB smears from naïve and immunized *NPMc* mice showing the presence of circulating atypical immature myeloid cells in the PB of immunized but not naïve transgenic mice. Scale bars, 20 μm.

Published OnlineFirst May 23, 2017; DOI: 10.1158/0008-5472.CAN-17-1098

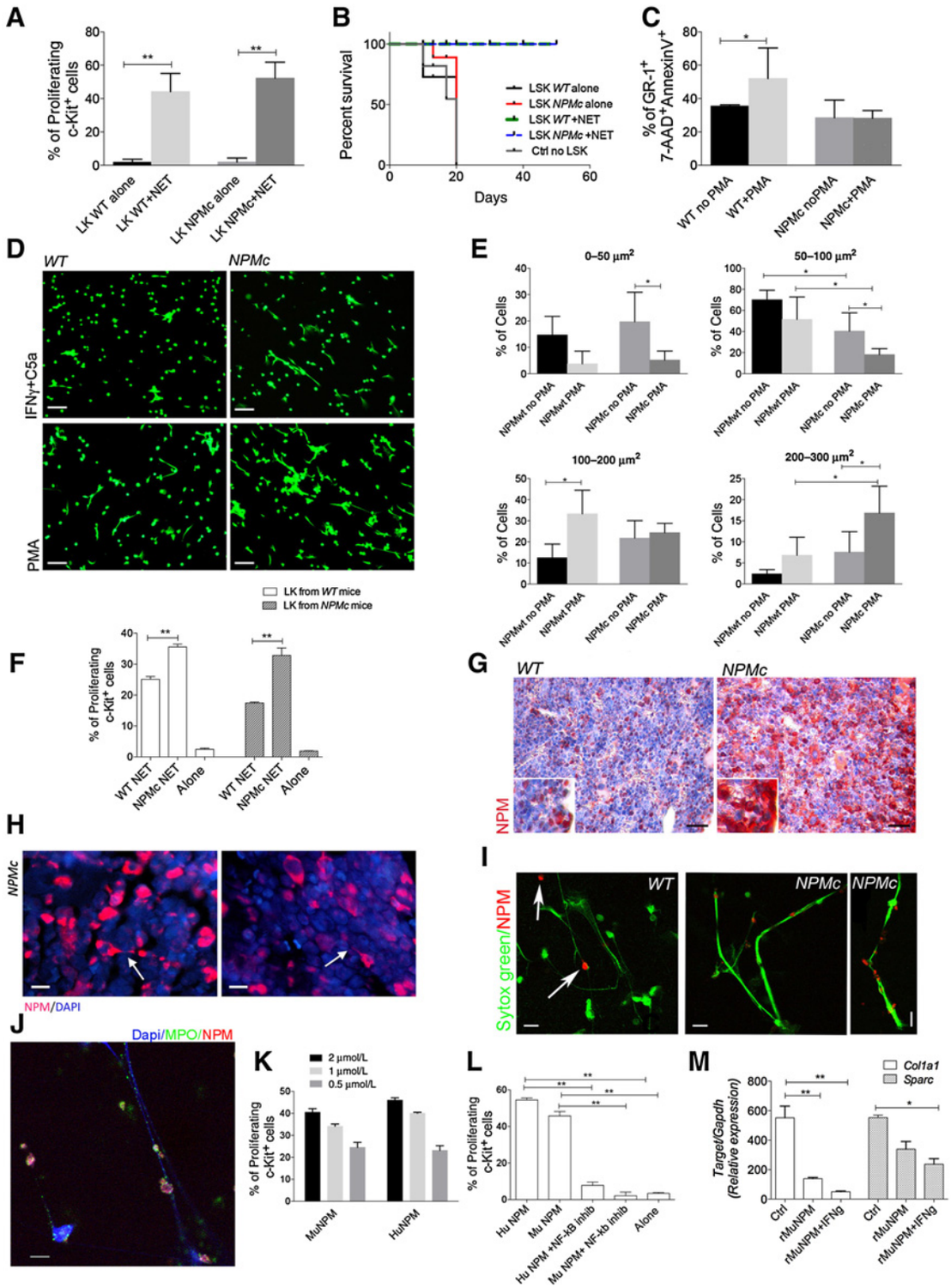

Figure 4.

NPMc mutation increases the proliferative response of hematopoietic precursors to NET stimulation. **A,** FACS-sorted Lin$^-$c-Kit$^+$ cells were isolated from *NPMc* and WT mice, cocultured with NETs, and evaluated for proliferation *in vitro.* The panel shows that the *NPMc* mutation does not confer a cell-intrinsic proliferative advantage to c-Kit$^+$ cells as the proliferative response to NET is comparable in the two genotypes. **B,** Lin$^-$Sca1$^+$Kit$^+$ cells from *NPMc* and WT mice were cocultured in the presence or absence of NET, without other supplements, and injected intravenously into lethally irradiated WT mice. All the mice receiving Lin$^-$Sca1$^+$Kit$^+$ cocultured with NETs survived independently from the *NPMc* genotype of the transplanted cells. (*Continued on the following page.*)

Published OnlineFirst May 23, 2017; DOI: 10.1158/0008-5472.CAN-17-1098

progenitors (GMP, MEP), megakaryocytes and megakaryocyte precursors in immunized *NPMc* mice. Conversely, the total number of B220$^+$ B cells decreased (Fig. 3G; Supplementary Fig. S5B for representative gating strategy).

Dysplastic features were also found in megakaryocytic and granulocytic cells within extramedullary splenic hematopoietic foci, which were expanded in immunized *NPMc* mice (Supplementary Fig. S6A). Indeed, the frequency of cytoplasmic NPM-expressing elements and of proliferating Ki67-expressing myeloid elements was increased in the spleen of immunized *NPMc* mice (Supplementary Fig. S6B–S6E). Flow cytometry analysis of spleen myeloid populations showed a significant expansion in the amount of LK cells and of granulocyte–monocyte progenitor (GMP) in immunized *NPMc* mice (Supplementary Fig. S6F–S6I). Finally, c-Kit$^+$ blasts had a higher frequency in the blood of immunized *NPMc* mice, a finding corroborated by the enrichment in morphologically immature circulating myeloid cells (Fig. 3H and I).

To provide an alternative approach testing the impact of persistent immune stimulation on the take of an established acute leukemia, we adopted the C1498 murine leukemia model (32). C57BL/6 mice were either immunized or not with DCs loaded with NET components and 1 month after the last immunization they were injected intra-bone with 2×10^5 GFP-labeled C1498 cells. Twenty-eight days after cell injection, mice were sacrificed and evaluated for the presence of C1498 in the bone marrow by FACS. Immunization significantly promoted the leukemic cell take in the bone marrow with the increased fraction of C1498 cells inversely correlating with that of B220$^+$ resident cells, which were outcompeted (Supplementary Fig. S7). These results indicate that systemic and persistent immune activation can exacerbate the phenotype of a genetically driven myeloproliferative spur.

NPMc mutation affects the NETosis of PMN and NET-induced proliferation of c-Kit$^+$ cells

Considering the data obtained in immunized *NPMc* mice, we hypothesized that NETs could confer a stronger proliferative advantage to hematopoietic precursors of *NPMc* rather than WT genotype. Unexpectedly, the presence of the *NPMc* mutation did not confer an intrinsic proliferative advantage to c-Kit$^+$ cells in response to NET stimulation (Fig. 4A). In line, LSK cells from *NPMc* and WT mice cocultured with NETs in the absence of any growth factor (i.e., SCF or IL3) were equally able to survive in culture and to reconstitute lethally irradiated mice (Fig. 4B).

We then investigated whether bone marrow myeloid cells from *NPMc* and WT mice were differently prone to NET formation. To this end, bone marrow PMNs isolated from *NPMc* and WT mice were seeded onto poly-D-lysine–coated slides and treated with IFNγ plus C5a or PMA. In both conditions, PMNs from *NPMc* mice showed a significantly increased NET formation in response to inflammatory stimuli (Fig. 4D and E). Moreover, NETs from *NPMc* mice were more efficient in enhancing proliferation of c-Kit$^+$ cells (Fig. 4F).

As NPM may act as an alarmin and contribute to systemic inflammation, for example, during sepsis (33), we hypothesized that the *NPMc* mutation, which causes cytoplasmic nucleophosmin localization (34), could be also responsible for its reallocation onto NETs, thereby influencing its availability as a NET-associated alarmin. IHC analyses performed on bone marrow sections showed that NPM, which is almost absent in mature bone marrow-PMNs of WT mice, is detectable in the cytoplasm of bone marrow PMNs from *NPMc* mice (Fig. 4G). In these mice, immunofluorescence on bone marrow sections using an anti-NPM Ab detecting both normal and mutated NPM, also highlighted NET threads (Fig. 4H). Moreover, at confocal microscopy, *ex vivo* NET from *NPMc* mice displayed NPM relocalized onto the NET DNA threads (Fig. 4I), where it associated with classical NET cytoplasmic proteins, such as MPO (Fig. 4J).

To test the ability of extracellular NPM to act as an alarmin for hematopoietic cells, LK cells were cultured in the presence of recombinant human and mouse NPM. As a result, proliferation of c-Kit$^+$ cells exposed to extracellular NPM was significantly enhanced in a dose-dependent manner and this effect could be inhibited by NF-κB blockade (Fig. 4K and L). Recombinant NPM mimicked TNF and IFNγ inflammatory stimuli in down-modulating the expression of ECM molecules in bone marrow-MSCs (Fig. 4M), a condition that promotes NET formation, delineating a self-sustaining inflammatory loop in AML carrying *NPM1* mutation.

(*Continued.*) **C,** Neutrophils were isolated from the bone marrow of *NPMc* and WT mice and treated with PMA for 24 hours. Upon PMA-mediated activation, *NPMwt* and *NPMc* PMNs exhibited a different rate of apoptosis, which was higher in the former group. **D,** Increased NET formation by *NPMc* mutant neutrophils compared with their *NPMwt* counterparts in response to IFNγ$^+$C5a or PMA activation (quantification is shown in Supplementary Fig. S10). Scale bars, 20 μm. **E,** Quantification of NET formation is shown for PMA-treated *NPMc* and WT neutrophils. Nuclear areas are plotted against the percentage of SYTOX-positive cells corresponding to a given nuclear area. PMN showing an enhanced propensity to undergo NETosis display an increased frequency of nuclei with highest nuclear areas. In this experiment, the SYTOX green DNA dye was added to PMN after PFA-fixation, 18 hours later. Experiments comparing PMN from *NPMc* transgenic or *WT* mice were repeated three times with PMN from at least three donor mice each. Number of nuclei analyzed/experiment = 200 (*, $P < 0{,}05$, Mann–Whitney *t* test). **F,** FACS-sorted Lin$^-$c-Kit$^+$ cells were isolated from the bone marrow of *NPMc* and *NPMwt* mice and cocultured with NETs obtained from *NPMc* and *NPMwt* mice. The image shows that *NPMc*-derived NETs promoted the proliferation of c-Kit$^+$ hematopoietic cells more efficiently in a 48 hours (instead of 72 hours) assay. **G,** IHC for NPM was performed on bone marrow sections from *NPMc* and *NPMwt* mice. The representative image shows that, in *NPMc* transgenic mice, cytoplasmic staining of NPM revealed hematopoietic myeloid cells, including mature granulocytes, scattered throughout the bone marrow interstitium. This was not observed in the bone marrow of the *NPMwt* mice. Scale bars, 50 μm. **H,** Immunofluorescence analysis of the bone marrow of *NPMc* mice showing that NPM is detected in association with MPO$^+$ DNA-thread structures suggestive of NET (arrows). Scale bars, 20 μm. **I,** Confocal immunofluorescence analysis for NPM performed in bone marrow neutrophils from *NPMwt* and *NPMc* mice seeded onto poly-D-lysine coated glasses and stimulated with PMA to induce NET formation. Staining for NPM (red signal) was performed without permeabilizing cells, which allowed detection of only NPM associated with extruded NET (highlighted by the DNA dye Sytox green, green signal) in *NPMc* neutrophils or apoptotic cells (arrow) in NPMwt neutrophils, but not NPM retained within live cells. In *NPMwt* neutrophils, NPM was not detected, except in apoptotic cells (arrows). Scale bars, 10 μm. **J,** Confocal microscopy analysis performed on NET from *NPMc* neutrophils showing NPM colocalizing with MPO, a classical NET-associated protein, onto the DNA (Dapi staining) threads. Scale bars, 10 μm. **K** and **L,** Proliferation of CFSE-labeled FACS-sorted Lin$^-$c-Kit$^+$ cells in response to recombinant murine and human NPM, with or without NF-κB inhibitor. Proliferation was evaluated at 72 hours ($n = 5$/group; **, $P < 0.01$, Mann–Whitney test). **M,** Expression of *Col1a* and *Sparc* genes in bone marrow-MSC stimulated or not with IFNγ, TNF, or their combination. The fold change in expression of the target genes relative to the internal control gene (GAPDH) is shown.

Published OnlineFirst May 23, 2017; DOI: 10.1158/0008-5472.CAN-17-1098

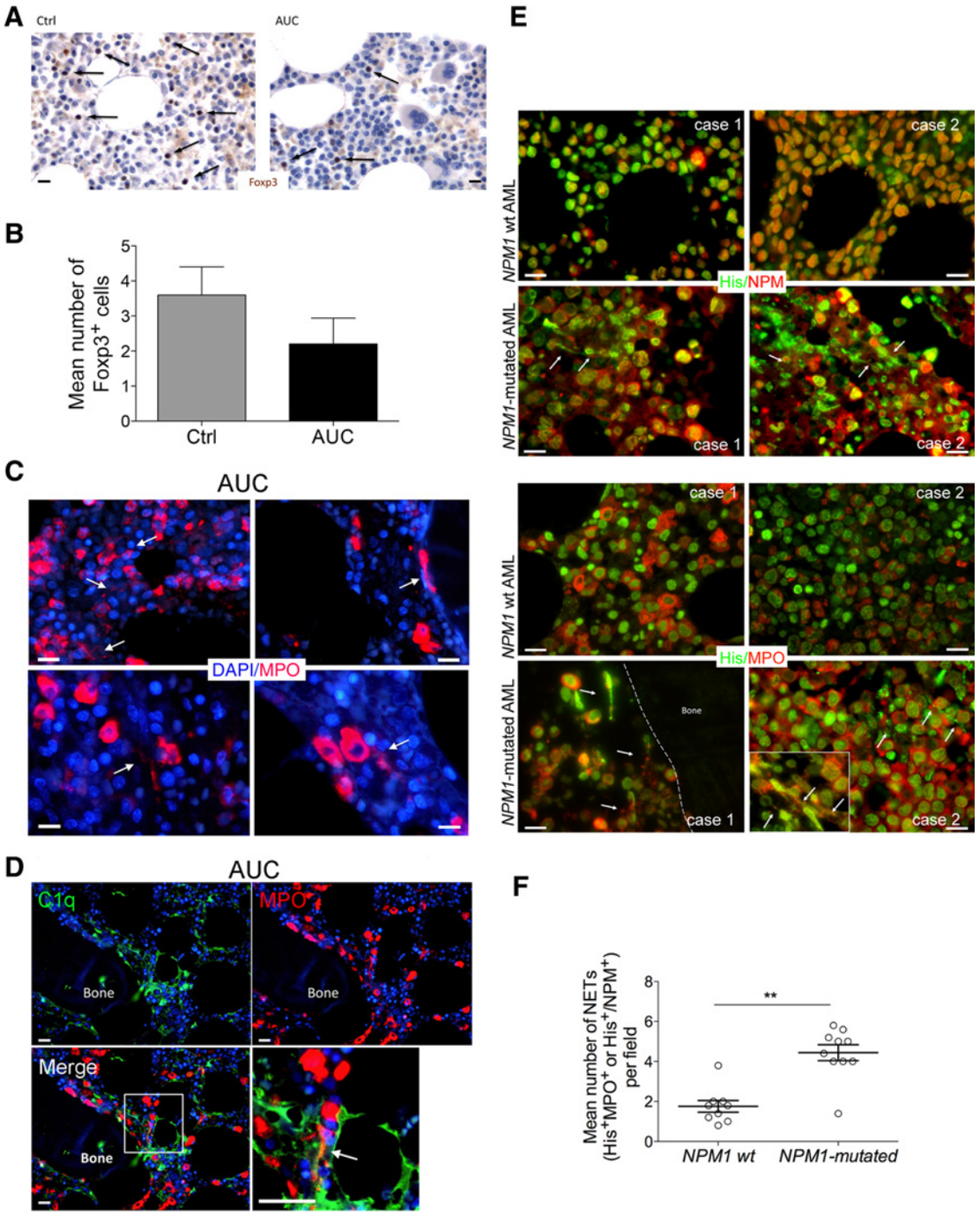

Figure 5.

In situ NET detection in autoimmune and *NPM1*-mutated AML patients. **A,** IHC analysis for Foxp3 performed on one representative case of autoimmune patient compared with healthy control. Foxp3$^+$ Treg, arrows. Scale bars, 20 μm. **B,** Mean number of Foxp3$^+$ cells in the bone marrow of autoimmune patients (cumulative data; $n = 5$/fields/patient; $n = 12$/group patients). Scale bars, 20 μm. **C,** Immunofluorescence for MPO of bone marrow sections from patients with autoimmunity-associated cytopenias (patients #4 and #9; Supplementary Table S1) showing the presence of extracellular MPO threads, suggestive of NET formation within the bone marrow interstitium. **D,** Representative immunofluorescence analysis of bone marrow from a patient with autoimmunity-associated cytopenia (patient #4, Supplementary Table S1) showing C1q complement deposition in bone marrow stromal cells and the close proximity between C1q$^+$ stromal elements (green) and NET MPO threads (red; arrow). Scale bars, 20 μm. **E,** Representative double-marker immunofluorescence microphotographs of WT and *NPM1*-mutated human AML bone marrow biopsies showing the presence of histone H3 threads (green signal) associated with either NPM (red signal, top) or MPO (red signal, bottom) in NET structures (arrows). NET histone H3 threads were prevalently detected in *NPM1*-mutated cases, in which NPM was relocalized into the cytoplasm. Scale bars, 20 μm. **F,** Mean number of NETs, evaluated as MPO$^+$ or NPM$^+$ histone H3$^+$ double positive threads, in bone marrow biopsies from WT and *NPM1*-mutated AML (for patient details, Supplementary Table S7).

Published OnlineFirst May 23, 2017; DOI: 10.1158/0008-5472.CAN-17-1098

In situ NET formation can be identified in patients with systemic autoimmunity and in AML patients with NPM1 mutation

To establish the translational significance of findings in experimental models, we performed studies in patients with systemic autoimmunity and in myeloid malignancies. Analysis of the bone marrow of patients with unexplained peripheral cytopenias and signs of systemic autoimmunity (AUC; Supplementary Table S1) showed mild alteration in granulocytic and megakaryocytic differentiation that did not configure impaired hematopoiesis or frank myelodysplasia when compared with normal controls (not shown). No significant differences were found in the overall amounts of bone marrow-infiltrating T cells; however, a trend towards the reduction of $Foxp3^+$ Treg cells was observed in the bone marrow of patients with autoimmune disorders (Fig. 5A and B). Most importantly, in these same patients, NETs were identified *in situ* by staining for MPO and DAPI (Fig. 5C). In patients with circulating autoantibodies (Supplementary Table S1), NET extracellular MPO threads were associated with C1q deposition (Fig. 5D).

We then investigated the presence of NETs in the bone marrow of AML patients carrying mutations in the *NPM1* gene. Immunofluorescence analysis for the chromatin marker Histone-H3 and either MPO or NPM was performed on 20 cases of AML with mutated ($N = 10$) or WT ($N = 10$) *NPM1*. We found that, in human AML cases, NETs were detected as Histone-$H3^+$ threads associated with MPO in cases in which MPO expression was preserved (Fig. 5E). As shown in transgenic *NPMc* mice, in the bone marrow of patients with *NPM1*-mutated AML, NET figures could be identified as characterized by the peculiar NPM localization onto the DNA thread marked by Histone-H3 (Fig. 5E). Quantification of NET figures as highlighted by Histone H3 and NPM or MPO on 5 high-power magnification microscopic fields, revealed that a higher frequency of NET figures could be identified in *NPM1* mutated cases (Fig. 5F; Supplementary Table S2). These data suggest that formation of NETs in the bone marrow observed in experimental systemic autoimmunity can be also observed in spontaneously occurring human autoimmune pathologies and occurs within the bone marrow environment of AML with mutated *NPM1*.

A NET-related inflammatory gene signature discriminates myeloid leukemia subsets

We then asked whether the inflammatory profile related with NETosis could be differently enriched at the transcriptional level in human myeloid malignancies.

To this end, we designed an *ad hoc* gene signature representative of the pathways activated in the bone marrow upon immunization and implicated in NET induction (Supplementary Table S3; ref. 5). The signature, thereafter referred to as NET-related inflammatory signature, was analyzed in a large panel of primary hematopoietic malignancies, including AML ($N = 100$), chronic myelogenous leukemia (CML, $N = 50$), MDS ($N = 50$), and in healthy bone marrow samples ($N = 30$), obtained from a large multicentric GEP study (see the Supplementary Information). Unsupervised hierarchical clustering based on the expression of the NET-related inflammatory signature separated AML samples from CML, MDS, and healthy bone marrow samples (Supplementary Fig. S8A). When a supervised approach was used to identify, within the NET-related inflammatory signature, the most suitable genes to differentiate the various diseases (ANOVA, $P < 0.05$, fold change > 2), AML was again separated from the other samples (Supplementary Fig. S8B).

Considering the variability in the NET-related inflammatory GEPs in AML, we investigated the AML cases in depth in order to understand the contribution of inflammation-related genes in this pathologic setting. We identified 20 genes (corresponding to 27 probe sets) belonging to the NET-related inflammatory signature that were differentially expressed in AML versus healthy bone marrow samples (*t*-test, $P < 0.05$, fold change >2; Supplementary Table S4). On the basis of the expression of these genes, AML cases could be divided into two clusters: cluster 1 and cluster 2 (Supplementary Fig. S8C). A supervised analysis (*t* test, $P < 0.05$; multiple testing correction: Bonferroni family wise error rate) was then performed to identify differentially expressed genes in cluster 1 and cluster 2. We identified 592 probe sets that enabled efficient discrimination between the two clusters (Supplementary Table S5; Fig. 6A). When studied by gene set enrichment analysis (GSEA) the corresponding 440 genes turned out to be significantly associated, as expected, with inflammation and immune response programs as well as with other relevant cellular processes and pathways, including some related with signal transduction, hematopoietic and leukemic stemness and, most notably, NPM1 signaling (Supplementary Table S6; Fig. 6B). This expression pattern was not found to be related to cytogenetic features in AML. Indeed, the two AML clusters comprised all different karyotypic groups (Supplementary Fig. S8D). Furthermore, the 17 genes (corresponding to 25 probe sets) belonging to the NET-related inflammatory signature, which were differentially modulated across the cytogenetic groups, as identified by supervised analysis (ANOVA, $P < 0.05$, fold change >2), were unable to clearly discriminate between AML cases with different karyotypic abnormalities (Supplementary Fig. S8E and S8F).

We extended the supervised analysis to an independent panel of 461 AML cases for which gene expression data, information on *NPM1* mutational status, and clinical follow-up were available (GEO Access: GSE6891; ref. 23). Again, the identified NET-related inflammatory signature defined two AML clusters in which mutated and wild-type *NPM1* cases were significantly segregated (χ^2, $P < 0.001$; Fig. 6C). Similar results were obtained by performing hierarchical clustering based on the expression of the 440 genes (Supplementary Table S5) discriminating the two AML clusters: *NPM1*-mutated and *NPM1*-wild type cases were significantly divided (χ^2, $P < 0.001$; Supplementary Fig. S8G). This pattern was independent from karyotype, in particular cases with normal karyotype were homogeneously distributed in the two clusters (χ^2, $P = 0.19$). Consistently, we found that differentially expressed genes in mutated versus wild-type *NPM1* cases were significantly enriched in the inflammatory response, IFNγ response, IL6 signaling, and complement cascade programs at gene set enrichment analysis (Supplementary Table S7). Conversely, when GEPs of cases presenting with somatic mutations affecting leukemia-associated genes other than *NPM1* (*CEBPA*, *IDH1*, *IDH2*, *KRAS*, *NRAS*, and *FLT3*-ITD) were investigated, *IDH1*-mutated cases were found to display significant enrichment in genes belonging to the NET-related signature, even if only very few cases ($N = 3$) among those of the analyzed panel had isolated *IDH1* mutations.

The NET-related inflammatory gene signature predicts response to immunomodulatory drugs

To assess the potential clinical impact of NET-related inflammatory features, we applied our signature to a cohort of high-risk

Published OnlineFirst May 23, 2017; DOI: 10.1158/0008-5472.CAN-17-1098

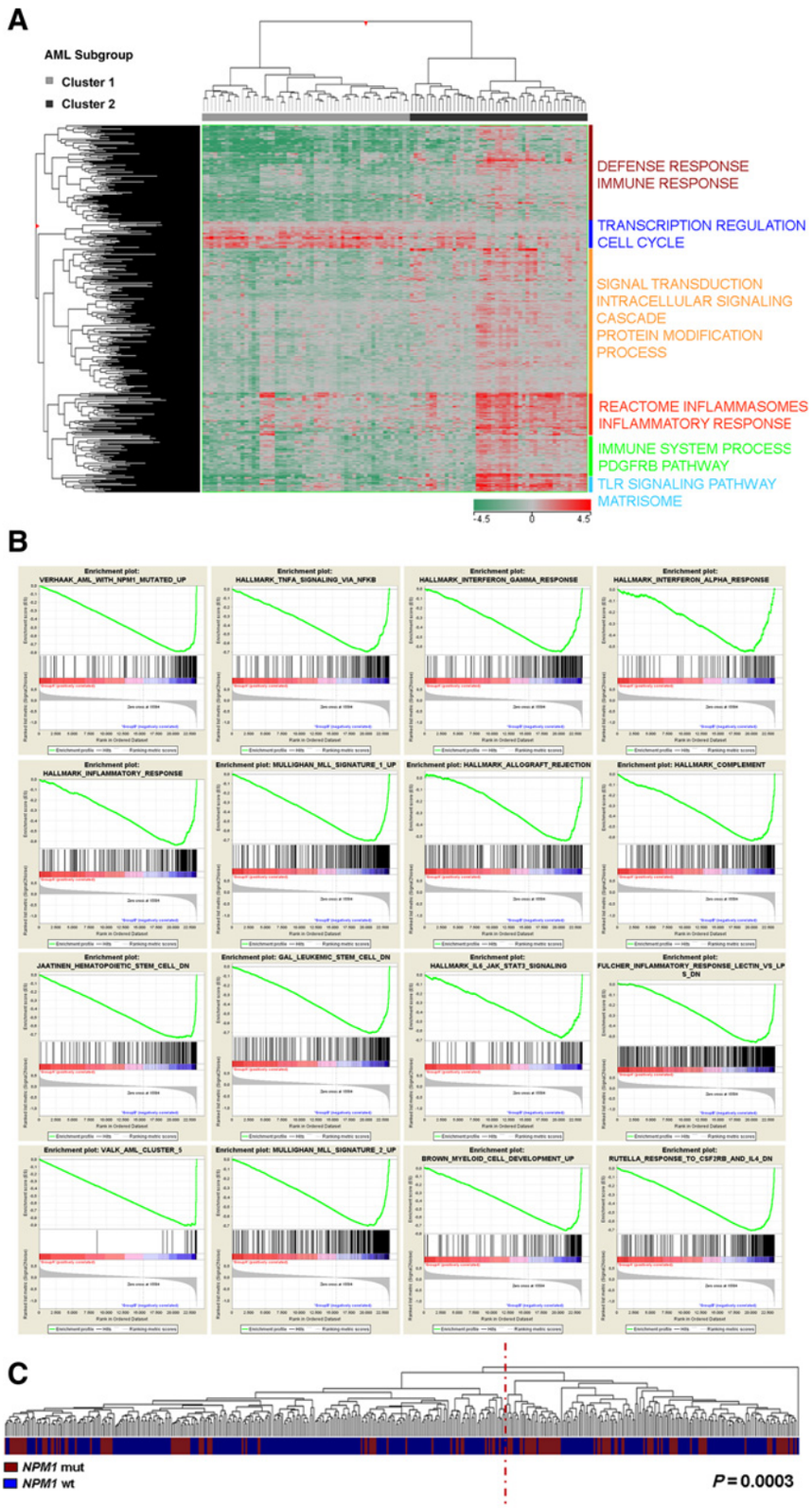

Figure 6.

A NET-related inflammatory gene signature subdivides acute myeloid leukemias **A,** Supervised analysis of AML cases divided by cluster (1 vs. 2) as defined by the expression of the NET-related inflammatory signature. The two clusters differ in the expression of 440 genes belonging to programs of inflammation, immune response, leukemic stemness, and, notably NPM-1 signaling. In the matrix, each column represents a sample and each row represents a gene. The color scale bar shows the relative gene expression changes normalized to the standard deviation (0 is the mean expression level of a given gene). The main Biological Processes (GeneOntology) identified by GSEA are highlighted on the right. **B,** GSEA of the differentially expressed genes in AML cluster 1 vs. AML cluster 2 showing the positive enrichment of diverse inflammatory programs in AML cluster 2. The enrichment score relative to the different datasets is shown. **C,** Hierarchical clustering of AML cases based on the NET-related inflammatory signature showing that *NMP1* mutated cases were significantly segregated (χ^2, $P < 0.001$) according to the signature.

Published OnlineFirst May 23, 2017; DOI: 10.1158/0008-5472.CAN-17-1098

AML patients ($N = 26$; complete responders = 14; nonresponders = 12) treated with the combination of chemotherapy and the immunomodulatory drug lenalidomide (24). The molecular signature associated with complete response (24) significantly overlapped with the NET-related inflammatory signature (χ^2, $P = 0.03$), being also enriched in genes characteristic of NPM1 mutated AML. In the same cohort of patients, the NET-related inflammatory signature enabled subdivision of the AML cases into two groups with significantly different overall survival (median estimated survival 1 month vs. 20 months; 95% confidence interval, 0.140–6.88/1.86–45.11 months; $P < 0.001$; Fig. 7A). A minimal signature consisting of three genes (Fig. 7B) belonging to the NET-related inflammatory signature, namely *IRF7*, *C5AR1*, and *NFKBIA*, were able to discriminate patients with a significantly better or worse outcome ($P = 0.03$; Fig. 7C). Taken together, these data showed that, although not associated with clinical outcome in a cohort of AML patients treated with conventional chemotherapy, the expression pattern of genes related with NETs was associated with the clinical response and survival of AML patients receiving the immunomodulatory agent lenalidomide.

Discussion

We showed that structural changes in the bone marrow stroma are involved in shaping the myeloproliferative bone marrow responses to systemic persistent immune stimulation. Immunization-induced autoimmunity was found to elicit downregulation of SPARC and type I collagen in the bone marrow stroma as well as to promote local inflammatory conditions associated with T-cell activation and NETosis.

Within the bone marrow, NET sustained the proliferation of hematopoietic precursors via the release of the hematopoietic cytokines SCF and IL6 involving NF-κB.

The discovery of NET-induced expansion of hematopoietic precursors prompted us to investigate whether the transcriptional profiles of various human myeloid malignancies were differently enriched in a NET-related gene signature. We found that AML were divided into two main clusters according to the inflammatory imprint. The inflammatory cluster segregated according to NPM1 mutation-associated molecular programs. The NPM1 mutation is the most frequent genetic alteration identified in acute myeloid leukemia (AML) accounting for

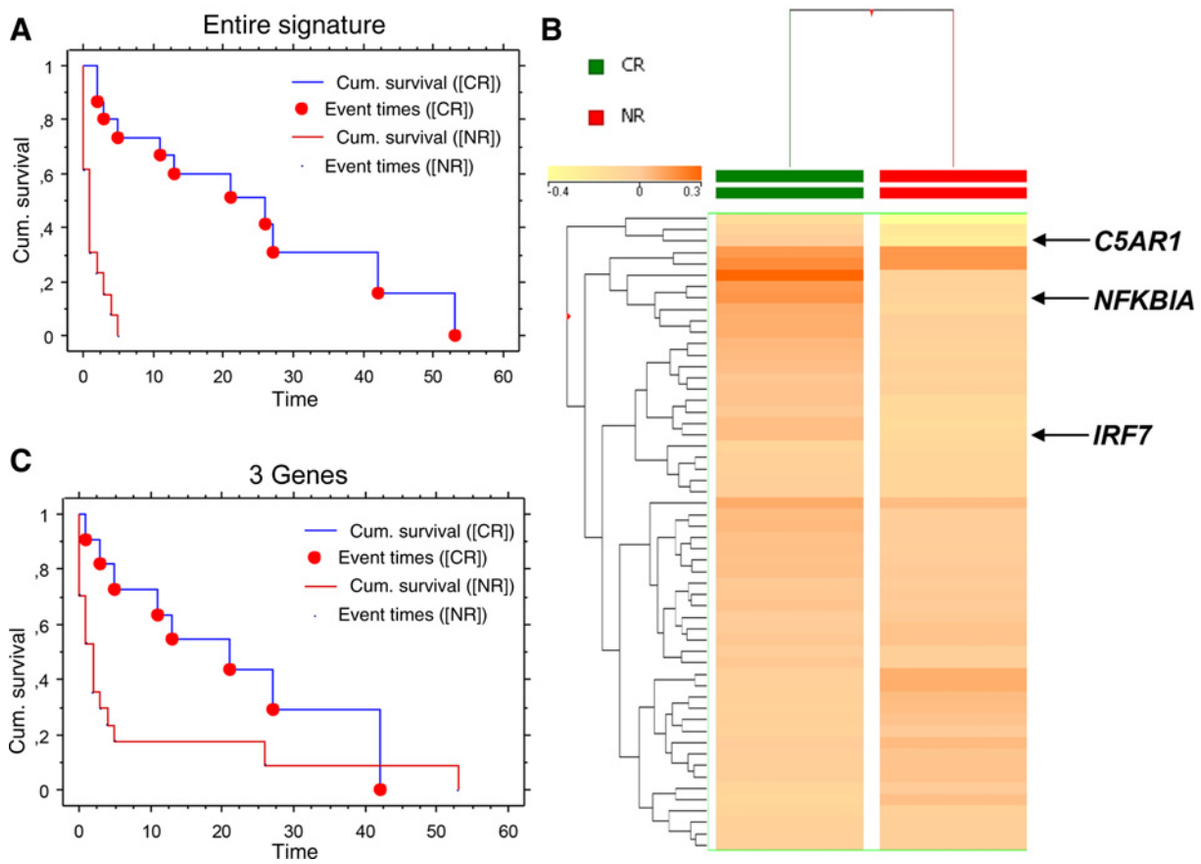

Figure 7.

The NET-related inflammatory gene signature predicts response to immunomodulatory drugs. **A,** OS curves (Kaplan–Meier method) of AML patients treated with lenalidomide plus AraC classified into two groups [group 1, complete responders (CR), blue line; group 2, nonresponders (NR), red line] based on the expression of the entire NET-related inflammatory signature (support vector machine algorithm). **B,** Three genes belonging to the NET-related inflammatory signature were found among those differentially expressed according to the clinical response (complete responders vs. nonresponders achievement) in AML patients receiving lenalidomide plus AraC (24). **C,** OS curves (Kaplan–Meier method) of AML patients treated with lenalidomide plus AraC classified into two groups (group 1, complete responders, blue line; group 2, nonresponders, red line) based on the three genes of the NET-related inflammatory signature (C5AR1, NFKBIA, IRF7; support vector machine algorithm).

Published OnlineFirst May 23, 2017; DOI: 10.1158/0008-5472.CAN-17-1098

about 30% of all cases. This mutation defines a subgroup of AML with distinctive clinicopathologic features and it is also associated with a unique GEP (18). The role of NPM1 mutation in leukemogenesis *in vivo* has not been fully elucidated. The low genetic complexity of NPM1-mutated AML suggests that this mutation requires additional stimuli, which might also be provided by the inflammatory microenvironment, to promote malignant clone progression (18).

In this context, a large study involving 1,540 patients has shown that the impact of *NPM1* mutation on transformation become manifested only in presence of initiating mutations in epigenetic pathways, such as in *DNMT3*, *TET2*, *IDH1/2* genes (35).

This makes no surprise that in the different transgenic (31) or conditional mouse model (36, 37), lacking addition mutations, a frank leukemia was rarely observed, although an indolent myeloproliferation, perturbed megakaryopoiesis, or MPD have been reported. However, investigating whether an inflammatory bone marrow environment was able to aggravate the indolent myeloproliferative phenotype of *NPMc* transgenic mice we found that features of dysplastic changes and increased extramedullary hematopoiesis were induced in *NPMc* immunized mice. The *NPMc* mutation cooperated with NET-mediated stimulation of c-Kit$^+$ precursors according to the propensity of *NPMc* PMN to NETosis and because of the alarmin function of the NET-complexed cytoplasmic mutated NPM. This may explain, at least in part, why the NET-related inflammatory signature was found to be enriched in AML with mutated *NPM1*. Accordingly, the mutated NPM, although aberrantly translocated to the cytoplasm, conserves its functional domains, including the histone-binding domains (38), which may explain its affinity for histone-rich NET DNA threads and its related pro-alarmin function. This suggests that *NPMc*-bearing clones may benefit from the presence of NET-triggering conditions, which may be irrelevant for clones with t(3,5) translocation (NPM1-MLF1) or loss of chromosome 5, which result in the loss of the DNA-binding domain or in the complete loss of NPM (39).

We discovered a novel role for NETs in stimulating hematopoietic precursor proliferation, also extending the influence of this form of myeloid cell death to hematopoiesis and related disorders. The identification of AML subgroups characterized by a NET-related inflammatory signature and bone marrow NET induction claims for the investigation of immunomodulatory agent-containing treatments to be adopted in combination with conventional therapy in selected patients.

Disclosure of Potential Conflicts of Interest

No potential conflicts of interest were disclosed.

Authors' Contributions

Conception and design: C. Tripodo, A. Liso, G. Visani, M.P. Colombo, S. Sangaletti

Development of methodology: C. Tripodo,

Acquisition of data (provided animals, acquired and managed patients, provided facilities, etc.): C. Tripodo, C. Chiodoni, P. Portararo, B Cappetti, L. Botti, A. Gulino, A. Isidori, A. Liso, G. Visani, M.P. Martelli, B. Falini, P.P. Pandolfi, S. Sangaletti

Analysis and interpretation of data (e.g., statistical analysis, biostatistics, computational analysis): C. Tripodo, A. Burocchi, P.P. Piccaluga, C. Chiodoni, A. Gulino, G. Visani, M.P. Martelli, B. Falini, S. Sangaletti

Writing, review, and/or revision of the manuscript: C. Tripodo, A. Burocchi, P.P. Piccaluga, A. Isidori, A. Liso, M.P. Colombo, S. Sangaletti

Administrative, technical, or material support (i.e., reporting or organizing data, constructing databases):

Study supervision: M.P. Colombo, S. Sangaletti

Acknowledgments

The authors thank Prof. Federica Sallusto (Institute for Research in Biomedicine, Università della Svizzera Italiana) and Prof. Niccolò Bolli (Fondazione IRCCS Istituto Tumori Milano and University of Milan) for critical reviewing of the manuscript. The authors also thank Professor Maurilio Ponzoni (Università Vita- Salute San Raffaele) and Professor Umberto Gianelli (Fondazione IRCCS Ca' Granda - Ospedale Maggiore Policlinico) for providing human tissue samples. The authors thank the Conventional and Confocal Microscopy Facility for confocal microscopy images acquisition, the Cell Sorting Facility for cell sorting, and Mrs. Ester Grande for administrative assistance.

Grant Support

This work was supported by the Associazione Italiana per la Ricerca sul Cancro (AIRC grant number 12810 to S. Sangaletti; Program Innovative Tools for Cancer Risk Assessment and Diagnosis, 5 per mille number 12162 to C. Tripodo and M.P. Colombo; investigator grant number10137 to M.P. Colombo), and the Italian Ministry of Health (GR-2013-02355637; to S. Sangaletti).

The costs of publication of this article were defrayed in part by the payment of page charges. This article must therefore be hereby marked *advertisement* in accordance with 18 U.S.C. Section 1734 solely to indicate this fact.

Received April 12, 2017; revised May 6, 2017; accepted May 8, 2017; published OnlineFirst May 23, 2017.

References

1. Kode A, Manavalan JS, Mosialou I, Bhagat G, Rathinam CV, Luo N, et al. Leukaemogenesis induced by an activating beta-catenin mutation in osteoblasts. Nature 2014;506:240–4.
2. Tripodo C, Di Bernardo A, Ternullo MP, Guarnotta C, Porcasi R, Ingrao S, et al. Cd146(+) bone marrow osteoprogenitors increase in the advanced stages of primary myelofibrosis. Haematologica 2009;94:127–30.
3. Della Porta MG, Malcovati L, Boveri E, Travaglino E, Pietra D, Pascutto C, et al. Clinical relevance of bone marrow fibrosis and Cd34-positive cell clusters in primary myelodysplastic syndromes. J Clin Oncol 2009;27:754–62.
4. Brekken RA, Sage EH. Sparc, A matricellular protein: at the crossroads of cell-matrix communication. Matrix Biol 2001;19:816–27.
5. Sangaletti S, Tripodo C, Vitali C, Portararo P, Guarnotta C, Casalini P, et al. Defective stromal remodeling and neutrophil extracellular traps in lymphoid tissues favor the transition from autoimmunity to lymphoma. Cancer Discov 2014;4:110–29.
6. Tefferi A, Vaidya R, Caramazza D, Finke C, Lasho T, Pardanani A. Circulating interleukin (IL)-8, IL-2R, IL-12, and IL-15 levels are independently prognostic in primary myelofibrosis: a comprehensive cytokine profiling study. J Clin Oncol 2011;29:1356–63.
7. Kornblau SM, Mccue D, Singh N, Chen W, Estrov Z, Coombes KR. Recurrent expression signatures of cytokines and chemokines are present and are independently prognostic in acute myelogenous leukemia and myelodysplasia. Blood 2010;116:4251–61.
8. Sangaletti S, Tripodo C, Cappetti B, Casalini P, Chiodoni C, Piconese S, et al. Sparc oppositely regulates inflammation and fibrosis in bleomycin-induced lung damage. Am J Pathol 2011;179:3000–10.
9. Sangaletti S, Tripodo C, Chiodoni C, Guarnotta C, Cappetti B, Casalini P, et al. Neutrophil extracellular traps mediate transfer of cytoplasmic neutrophil antigens to myeloid dendritic cells toward anca induction and associated autoimmunity. Blood 2012;120:3007–18.

10. Kessenbrock K, Krumbholz M, Schonermarck U, Back W, Gross WL, Werb Z, et al. Netting neutrophils in autoimmune small-vessel vasculitis. Nat Med 2009;15:623–5.
11. Garcia-Romo GS, Caielli S, Vega B, Connolly J, Allantaz F, Xu Z, et al. Netting neutrophils are major inducers of type I IFN production in pediatric systemic lupus erythematosus. Sci Translat Med 2011;3:73ra20.
12. Swerdlow SH, Campo E, Harris NL, Jaffe ES, Pileri SA, Stein H, et al. WHO classification of tumours of haematopoietic and lymphoid tissues, fourth edition. Lyon, France: IARC; 2008.
13. Schauer C, Janko C, Munoz LE, Zhao Y, Kienhofer D, Frey B, et al. Aggregated neutrophil extracellular traps limit inflammation by degrading cytokines and chemokines. Nat Med 2014;20:511–7.
14. Kristinsson SY, Bjorkholm M, Hultcrantz M, Derolf AR, Landgren O, Goldin LR. Chronic immune stimulation might act as a trigger for the development of acute myeloid leukemia or myelodysplastic syndromes. J Clin Oncol 2011;29:2897–903.
15. Lande R, Ganguly D, Facchinetti V, Frasca L, Conrad C, Gregorio J, et al. Neutrophils activate plasmacytoid dendritic cells by releasing self-DNA-peptide complexes in systemic lupus erythematosus. Sci Translat Med 2011;3:73ra19.
16. Fuchs TA, Abed U, Goosmann C, Hurwitz R, Schulze I, Wahn V, et al. Novel cell death program leads to neutrophil extracellular traps. J Cell Biol 2007;176:231–41.
17. Metzler KD, Fuchs TA, Nauseef WM, Reumaux D, Roesler J, Schulze I, et al. Myeloperoxidase is required for neutrophil extracellular trap formation: implications for innate immunity. Blood 2011;117:953–9.
18. Falini B, Mecucci C, Tiacci E, Alcalay M, Rosati R, Pasqualucci L, et al. Cytoplasmic nucleophosmin in acute myelogenous leukemia with a normal karyotype. N Engl J Med 2005;352:254–66.
19. Oostendorp RA, Audet J, Eaves CJ. High-resolution tracking of cell division suggests similar cell cycle kinetics of hematopoietic stem cells stimulated in vitro and in vivo. Blood 2000;95:855–62.
20. Kohlmann A, Kipps TJ, Rassenti LZ, Downing JR, Shurtleff SA, Mills KI, et al. An international standardization programme towards the application of gene expression profiling in routine leukaemia diagnostics: the microarray innovations in leukemia study prephase. Br J Haematol 2008;142:802–7.
21. Haferlach T, Kohlmann A, Wieczorek L, Basso G, Kronnie GT, Bene MC, et al. Clinical utility of microarray-based gene expression profiling in the diagnosis and subclassification of leukemia: report from the international microarray innovations in leukemia study group. J Clin Oncol 2010; 28:2529–37.
22. Verhaak RG, Wouters BJ, Erpelinck CA, Abbas S, Beverloo HB, Lugthart S, et al. Prediction of molecular subtypes in acute myeloid leukemia based on gene expression profiling. Haematologica 2009;94:131–4.
23. De Jonge HJ, Valk PJ, Veeger NJ, Ter Elst A, Den Boer ML, Cloos J, et al. High VEGFC expression is associated with unique gene expression profiles and predicts adverse prognosis in pediatric and adult acute myeloid leukemia. Blood 2010;116:1747–54.
24. Visani G, Ferrara F, Di Raimondo F, Loscocco F, Sparaventi G, Paolini S, et al. Low-dose lenalidomide plus cytarabine induce complete remission that can be predicted by genetic profiling in elderly acute myeloid leukemia patients. Leukemia 2014;28:967–70.
25. Long SA, Buckner JH. Cd4+Foxp3+ T regulatory cells in human autoimmunity: more than a numbers game. J Immunol 2011;187:2061–6.
26. Piconese S, Pittoni P, Burocchi A, Gorzanelli A, Care A, Tripodo C, et al. A non-redundant role for Ox40 in the competitive fitness of treg in response to Il-2. Eur J Immunol 2010;40:2902–13.
27. Martinelli S, Urosevic M, Daryadel A, Oberholzer PA, Baumann C, Fey Mf, et al. Induction of genes mediating interferon-dependent extracellular trap formation during neutrophil differentiation. J Biol Chem 2004;279: 44123–32.
28. Brinkmann V, Reichard U, Goosmann C, Fauler B, Uhlemann Y, Weiss Ds, et al. Neutrophil extracellular traps kill bacteria. Science 2004;303:1532–5.
29. Okada S, Nakauchi H, Nagayoshi K, Nishikawa S, Miura Y, Suda T. In vivo and in vitro stem cell function of C-Kit- and sca-1-positive murine hematopoietic cells. Blood 1992;80:3044–50.
30. Bottero V, Withoff S, Verma IM. NF-κB and the regulation of hematopoiesis. Cell Death Differ 2006;13:785–97.
31. Cheng K, Sportoletti P, Ito K, Clohessy JG, Teruya-Feldstein J, Kutok JL, et al. The cytoplasmic npm mutant induces myeloproliferation in a transgenic mouse model. Blood 2010;115:3341–5.
32. Zhang L, Gajewski TF, Kline J. Pd-1/Pd-L1 interactions inhibit antitumor immune responses in a murine acute myeloid leukemia model. Blood 2009;114:1545–52.
33. Nawa Y, Kawahara K, Tancharoen S, Meng X, Sameshima H, Ito T, et al. Nucleophosmin may act as an alarmin: implications for severe sepsis. J Leukoc Biol 2009;86:645–53.
34. Falini B, Bolli N, Shan J, Martelli Mp, Liso A, Pucciarini A, et al. Both carboxy-terminus nes motif and mutated tryptophan(S) are crucial for aberrant nuclear export of nucleophosmin leukemic mutants In Npmc+ Aml. Blood 2006;107:4514–23.
35. Papaemmanuil E, Gerstung M, Bullinger L, Gaidzik VI, Paschka P, Roberts ND, et al. Genomic classification and prognosis in acute myeloid leukemia. N Engl J Med 2016;374:2209–21.
36. Sportoletti P, Varasano E, Rossi R, Bereshchenko O, Cecchini D, Gionfriddo I, et al. The human Npm1 mutation a perturbs megakaryopoiesis in a conditional mouse model. Blood 2013;121:3447–58.
37. Vassiliou GS, Cooper JL, Rad R, Li J, Rice S, Uren A, et al. Mutant nucleophosmin and cooperating pathways drive leukemia initiation and progression in mice. Nat Genet 2011;43:470–5.
38. Falini B, Nicoletti I, Bolli N, Martelli MP, Liso A, Gorello P, et al. Translocations and mutations involving the nucleophosmin (Npm1) gene in lymphomas and leukemias. Haematologica 2007;92:519–32.
39. Grisendi S, Bernardi R, Rossi M, Cheng K, Khandker L, Manova K, et al. Role of nucleophosmin in embryonic development and tumorigenesis. Nature 2005;437:147–53.

Cancer Research
The Journal of Cancer Research (1916–1930) | The American Journal of Cancer (1931–1940)

AACR American Association for Cancer Research

Persistent Immune Stimulation Exacerbates Genetically Driven Myeloproliferative Disorders via Stromal Remodeling

Claudio Tripodo, Alessia Burocchi, Pier Paolo Piccaluga, et al.

Cancer Res 2017;77:3685-3699. Published OnlineFirst May 23, 2017.